Edith Cowan University

Research Online

Research outputs 2022 to 2026

10-1-2023

A review of the mechanical properties of 17-4PH stainless steel produced by bound powder extrusion

Jaidyn Jones

Ana Vafadar
Edith Cowan University

Reza Hashemi

Follow this and additional works at: https://ro.ecu.edu.au/ecuworks2022-2026

 Part of the Engineering Commons

10.3390/jmmp7050162
Jones, J., Vafadar, A., & Hashemi, R. (2023). A review of the mechanical properties of 17-4PH stainless steel produced by bound powder extrusion. Journal of Manufacturing and Materials Processing, 7(5), article 162. https://doi.org/10.3390/jmmp7050162
This Journal Article is posted at Research Online.
https://ro.ecu.edu.au/ecuworks2022-2026/3229

Journal of
Manufacturing and Materials Processing

MDPI

Review

A Review of the Mechanical Properties of 17-4PH Stainless Steel Produced by Bound Powder Extrusion

Jaidyn Jones [1], Ana Vafadar [2] and Reza Hashemi [1,*]

[1] College of Science and Engineering, Flinders University, Tonsley, SA 5042, Australia; jone0883@flinders.edu.au
[2] School of Engineering, Edith Cowan University, Joondalup, WA 6027, Australia; a.vafadar@ecu.edu.au
* Correspondence: reza.hashemi@flinders.edu.au

Abstract: 17-4PH Stainless Steel is a mechanically high-performing alloy that is widely used across chemical and mechanical processing industries. The alloy is conventionally fabricated by cast methods, but emerging additive manufacturing techniques are presently offering an economic, efficient, and environmentally friendly alternative. Bound Powder Extrusion (BPE) is a relatively new additive manufacturing technique that is used to fabricate three-dimensional, free-form components. Investigation into the mechanical properties and behavior of 17-4PH stainless steel fabricated by BPE is vital to understanding whether this technique proposes a competitive substitute to the cast alloy within industry. Published literature has investigated the as-fabricated mechanical properties, microstructure, porosity, and post-processing heat treatment of the BPE alloy, with limited comparison evident among the papers. This paper, therefore, aims to review published findings on the mechanical properties of 17-4PH stainless steel produced by additive manufacturing techniques, with a key focus on BPE. It is important to highlight that this review study focuses on the MetalX^{TM} 3D printer, manufactured by Markforged. This printer is among the widely utilized BPE 3D printers available in the market. The key results, together with the impact of post-heat treatments, were discussed and compared to provide a more comprehensive picture of the patterns that this alloy presents in terms of its microstructure and mechanical properties. This enables the manufacture of components relative to desired material performance, improving overall functionality. A comparison of yield strength, ultimate tensile strength (UTS), Young's modulus, ductility, and hardness was made relative to microstructure, porosity, and density of published literature for the as-fabricated and post-heat-treated states, identifying areas for further research.

Keywords: additive manufacturing; 17-4PH stainless steel; mechanical properties; post-heat treatment; Markforged MetalX^{TM}

check for updates

Citation: Jones, J.; Vafadar, A.; Hashemi, R. A Review of the Mechanical Properties of 17-4PH Stainless Steel Produced by Bound Powder Extrusion. *J. Manuf. Mater. Process.* **2023**, *7*, 162. https://doi.org/10.3390/jmmp7050162

Academic Editor: Mario Buchely

Received: 5 July 2023
Revised: 7 August 2023
Accepted: 16 August 2023
Published: 8 September 2023

Copyright: © 2023 by the authors. Licensee MDPI, Basel, Switzerland. This article is an open access article distributed under the terms and conditions of the Creative Commons Attribution (CC BY) license (https://creativecommons.org/licenses/by/4.0/).

1. Introduction

Metal additive manufacturing (AM) has revolutionized the manufacturing industry, achieving process efficiency, complex geometries, and environmental benefits such as reduced processing energy and material waste in contrast to conventional manufacturing practices of forging, casting, and machining [1]. The evolution of technology has propelled AM application from rapid prototyping to contributing a key role in the fourth industrial revolution (Industry 4.0), providing an opportunity for the customized design and optimized performance for a variety of materials, including composites, metals, and material hybrids [2,3]. Metal AM utilizes layer-by-layer methodologies categorized according to material, deposition technique, or process of material fusion or solidification [4]. Additive manufacturing of metallic materials comprises seven main groups, all of which have commercial applications in the metal AM market. Three commonly used AM techniques for metals are Material Extrusion (ME), Powder Bed Fusion (PBF), and Direct Energy Deposition (DED) [5]. ME involves the deposition of heated material onto a platform through chemical layer adhesion or controlled temperature, utilizing a continuous stream

and constant pressure. PBF distributes powder material over a platform and successive layers melted by a laser or electron beam to establish component fusion [6]. The process of DED comparatively utilizes a laser, electron beam, or arc to melt wire or powder feedstock and deposit it onto a multi-axial platform that uniquely offers layer fabrication at any angle. These standardized categories have been established by the American Society for Testing and Materials (ASTM), yet emerging technologies utilize a hybrid of processes and often contain attributes of more than one category to optimize their process and result [7].

17-4PH Stainless Steel, also known as AISI Grade 630, is a precipitation-hardening martensitic stainless steel that is widely used in various applications such as chemical processing equipment, fasteners, ball bearings, gears, and pump shafts owing to its great mechanical properties and corrosion resistance [8]. Conventional manufacturing and post-processing of this stainless steel achieves properties desirable for industry application, but at a cost of low machinability and high variance in microstructure [9,10]. As an alternative to conventional manufacturing, 17-4PH Stainless steel can be also fabricated by various metal AM techniques of Selective Laser Melting (SLM) by PBF, DED of Laser and Plasma Metal Deposition (LMD, PMD), and ME of Bound Powder Extrusion (BPE) and Fused Filament Fabrication (FFF) [11]. As fabricated, the AM material may vary significantly in microstructure and mechanical properties among techniques, and in comparison to wrought. Application of post-heat treatment can increase microstructural homogeneity and adjust mechanical properties, comparable to the industry-acceptable standard for the wrought alloy [12]. Optimization of the mechanical properties of additively manufactured 17-4PH stainless steel may be achievable through various post-processing treatments including Hot Isostatic Pressing (HIP), solution treatment, and direct aging, unique to each technique [13]. The mechanical properties attained by BPE demonstrate a competitive profile and material characteristics to the wrought material. BPE is a combination of FFF and Metal Injection Molding (MIM), producing a hybrid technique of Atomic Diffusion Additive Manufacturing (ADAM) that falls within the AM category of ME [14]. Markforged's BPE MetalX^{TM} system comprises a three-step process to produce an end-user product. Material is first extruded by a combination of fine metallic powder and waxy polymer through a nozzle layer by layer in a fashion nearly identical to conventional ME printing, fabricating a "Green Part". This is followed by the processing of a wash cycle to establish a de-bound "Brown Part", and finally processing through a sintering cycle to remove the adhesive polymer and subsequent porosity, producing the "Final Part" [15]. Previous studies report the beneficial impact of post-processing treatments on the MetalX^{TM} 17-4PH stainless steel to achieve comparable yield and tensile strengths to wrought, and superior properties of ductility, hardness, and porosity [16].

This paper aims to review published findings on the mechanical properties of 17-4PH Stainless Steel produced by additive manufacturing techniques, with a key focus on Markforged's MetalX^{TM}. The main results together with the impact of post-heat treatments are discussed and compared to provide a more comprehensive picture of the patterns that this alloy presents in terms of its microstructure and mechanical properties leading to a suitable selection of this AM stainless steel for various applications for better performance and functionality.

2. As-Fabricated Mechanical Properties of 17-4PH Stainless Steel

The as-fabricated mechanical properties of 17-4PH Stainless Steel are necessary to outline and discuss to establish the minimal performance expectations of the alloy. This further enables a comparison of material properties achieved by post-processing treatments, outlining the potential properties the alloy can achieve and recommendations for areas of further research. The mechanical properties of cast and AM 17-4PH stainless steel in their as-fabricated states are compared relative to yield strength, Ultimate Tensile Strength (UTS), Young's modulus, ductility, hardness, and density, demonstrating high variance in UTS, Young's modulus, and hardness. The as-fabricated state of the cast alloy is established in its annealed condition, also referred to as "condition A". This is achieved through

sintering the cast alloy at 1040 °C to 1065 °C, attaining a chemical composition of major elements 15–17.5% Chromium (Cr), 3–5% Nickel (Ni), and 3–5% Copper (Cu) [17]. The chemical composition standard of this alloy varies slightly per country; however, once annealed, there is little variance in the mechanical property performance. The mechanical properties of as-fabricated Grade 630 castings are given in Table 1, demonstrating its high mechanically performing capability [18,19]. Fabrication of 17-4PH Stainless Steel by the Markforged MetalX™ system achieves an as-fabricated state post-sintered, comparable to the wrought annealed condition. The sintering process involves heat treatment to 1300 °C, attaining a chemical composition corresponding to the wrought counterpart of 15–17% Cr, 3–5% Ni, and 3–5% Cu [20]. Markforged published data on the mechanical properties of the as-fabricated alloy is detailed in Table 1, printed by the MetalX™ system horizontal to the build plate. In the as-fabricated state, the MetalX™ alloy achieves increased UTS and hardness in comparison to the wrought.

Table 1. Mechanical properties of Grade 630 (17-4PH Stainless Steel) Cast, MetalX™ BPE, Laser PBF, MIM, and FFF.

Mechanical Properties	Grade 630 Casting [18,19]	MetalX™ BPE—Horizontal [20,21]	MetalX™ BPE—Vertical [22]	Laser PBF [23,24]	MIM [25]	FFF [26,27]
Yield Strength	760 MPa	710 MPa	476 MPa	460 MPa	689 MPa	900 MPa
UTS	1030 MPa	1180 MPa	554 MPa	1150 MPa	1000 MPa	800–1160 MPa
Young's modulus	196 GPa	152 GPa	107 GPa	137 GPa	190 GPa	160 GPa
Ductility	8%	7%	0.5%	8%	8.5%	6%
Hardness	33 HRC	36 HRC	36 HRC	36 HRC	33 HRC	22 HRC
Relative Density	-	96.4%	96.4%	99%	98.2%	98%

Literature findings indicate deviance of up to 10% lower in UTS, ductility, and hardness, owing to the high porosity observed in the as-fabricated states. Material fracture has been observed to occur, primarily at the interface between filaments, indicating weakness in layer fusion of the MetalX™ system [21,22,28,29]. Literature investigating the anisotropic nature of the BPE technique has identified a high variance in as-fabricated mechanical properties relative to build orientation. Horizontally oriented specimens aligned to the build direction achieve optimal mechanical properties, corresponding to the results published by Markforged [21,28]. Vertically fabricated specimens demonstrate significant variance in yield strength, UTS, and ductility, owing to the high porosity and weakened material layer fusion in the plane of the specimen cross-sectional area [22]. The stress-strain curve relative to the build orientation from horizontal to vertical specimens, aligning to build direction is displayed in Figure 1a, capturing a property trend of the 60° oriented specimen lowest in UTS and ductility [22,30]. Figure 1b displays the specimen print orientations corresponding to the stress-strain curve findings in Figure 1a. The tensile strength relationship to build orientation in this plane is largely dependent on the filament interface and fusion; the tensile strength of the 60° to 90° oriented specimen demonstrates significant porosity defects, reducing the cross-sectional area and decreasing the tensile strength [22]. The geometry of these pores is discussed later, owing to the variance in tensile performance from 60° to 90°. In addition to tensile strength, the layer-by-layer methodology of the BPE technique typically results in residual stresses that adversely impact the component's structural integrity [30]. Kauffman et al. [15] investigated the geometric deviation of the input CAD file to the as-fabricated MetalX™ component. Three-dimensional scanning of the as-fabricated component identified the dimensions were typically within 0.81 mm of the as-designed component but detected up to 1.25 mm deviance horizontally [15]. Surface treatment of the as-fabricated components achieves a reduction in residual stresses; vertical as-fabricated specimens can achieve improved UTS measuring up to 1000 MPa and suggesting proportionate impact of surface roughness on tensile strength [23,28,30,31].

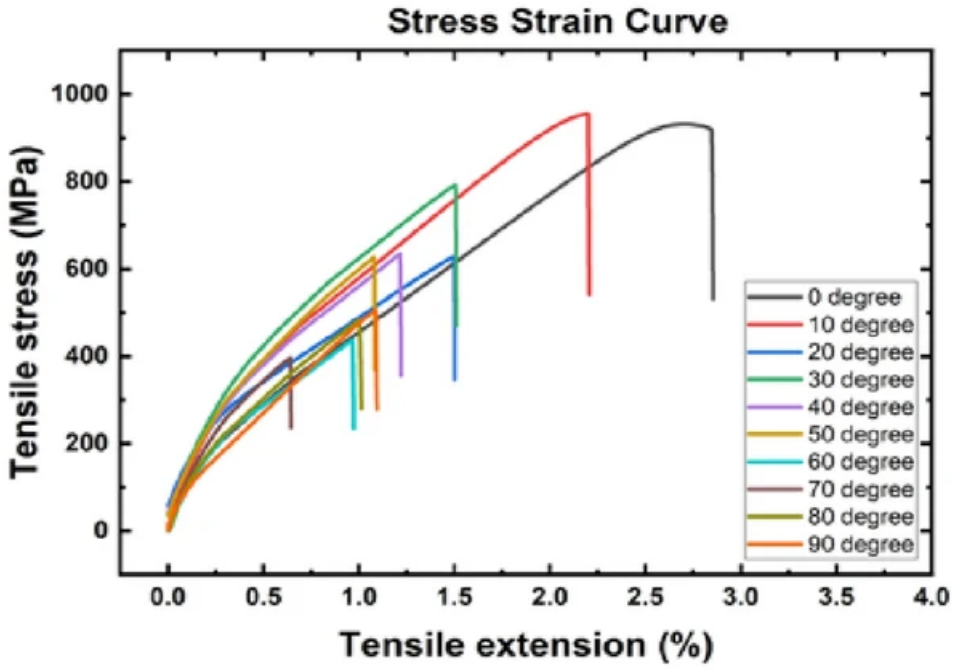

(**a**)

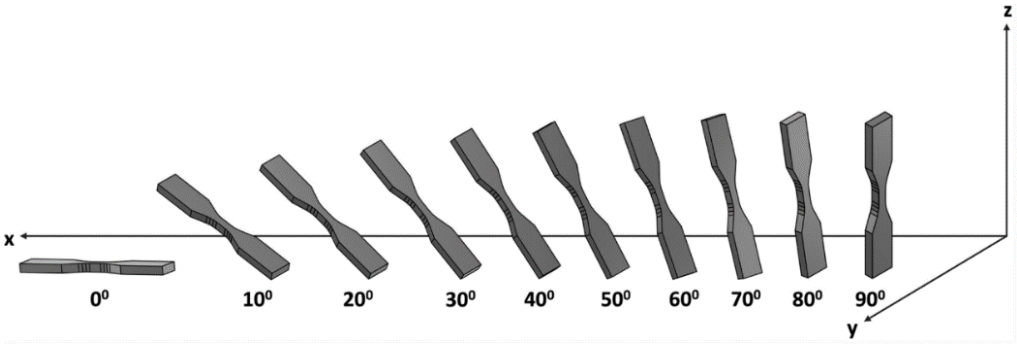

(**b**)

Figure 1. (**a**) As-fabricated mechanical properties of AM 17-4PH stainless steel relative to build angle, and (**b**) Specimen build orientations [22].

Life cycle impact assessment results based on Global Warming Potential (GWP) and Cumulative Energy Demand (CED) found significant benefits to the recyclability of the BPE alloy. The printing and sintering phases attributed 80% of the total environmental impact due to the high electricity consumption. The GWP and CED survey results are given in Table 2, outlining the minimal effect of post-processing on the overall processes' environmental impact [32].

Table 2. Environmental Impact Assessment Survey Results for BPE 17-4PH Stainless Steel Alloy [32].

	Global Warming Potential (kg Co_2 eq)		**Cumulative Energy Demand (MJ)**	
	As Fabricated	**Aged**	**As Fabricated**	**Aged**
Total	5.45	5.70	98.94	103.29
3D Printing	2.34	2.34	40.46	40.46
Debinding	0.28	0.28	6.15	6.15
Input Materials	0.68	0.68	9.95	9.95
Sintering	2.41	2.41	44.58	44.58
EoL	−0.17	−0.17	−2.06	−2.06
Heat Treatment	-	0.25	-	4.35

The as-fabricated mechanical properties of 17-4PH stainless steel fabricated by alternate AM techniques vary in comparison to MetalX^{TM}, relative to the deposition method. Literature findings of Laser PBF demonstrate equivalent improved hardness to the MetalX^{TM}, but lower UTS [24,33]. The mechanical properties are optimized through the use of water-atomized power, in comparison to gas-atomized powder, which achieves up to 10% and 27% less, respectively [34]. Further research has demonstrated a proportionate relationship between UTS, hardness, and density, with higher material density improving the mechanical performance of the components [26,27]. Published literature on FFF details high variance in mechanical properties attained, particularly in UTS. The findings exhibit higher performing yield strengths, but lower hardness and ductility [25,27]. The different sintering process parameters and the two debinding methods of catalytic or solvent based on the FFF technique affect the properties of the part such as porosity, microstructure, grain size, and amount of δ-ferrite. These proprieties are responsible for the dissimilar tensile strength and hardness values observed respective to known relationships for the stainless steel alloy [35,36]. Investigation into the effect of build angle demonstrated vertically oriented specimens relative to the build platform achieve lower tensile strength due to weakness in layer fusion, corresponding to the MetalX^{TM} findings; however, demonstrating improved fusion capability through achieving a UTS of 650 MPa [6,25]. Subsequently, published data on the as-fabricated mechanical properties achieved by MIM displays lower tensile strength, but the highest achieved ductility across the cast and metal AM data [37]. In contrast to Laser PBF, MIM attained optimized mechanical properties with a gas-atomized powder in comparison to water-atomized powder which achieved slightly lower mechanical properties [37,38]. This suggests the mechanical properties achieved by the MetalX^{TM} process could further be optimized by considering alternate types of input metallic powder.

The as-fabricated mechanical properties of the MetalX^{TM} 17-4PH stainless steel demonstrate competitive mechanical performance in comparison to other AM technologies and improved UTS and hardness to the wrought counterpart. Significant variation is found in yield strength and Young's modulus for the as-fabricated states, with corresponding results for ductility. The alternate AM technologies highlighted produced comparable mechanical performance to the MetalX^{TM} system in UTS, hardness, and ductility. In particular, FFF demonstrated higher yield strength and Young's Modulus to the MetalX^{TM} and MIM of higher ductility.

3. As-Fabricated Microstructure and Porosity of 17-4PH Stainless Steel

The mechanical behavior of cast and AM 17-4PH stainless steel can be examined through analysis of material characteristics and porosity. The cast alloy achieves its mechanically high-performing properties due to its martensitic microstructure formed by continuous annealing within the austenite region and rapid cooling [39,40]. Figure 2 displays Transmission Electron Microscopy (TEM) imaging [13], capturing the lath martensitic microstructure of the cast material. Literature findings have identified evident porosity as a result of the inadequate backfilling of liquid metal and solidification shrinkage throughout the casting process, causing significant variance in mechanical performance [41]. UTS and yield strength proportionately decrease relative to the reduction in load-bearing cross-section, and ductility decreases up to 80% with a 10% increase in porosity [41]. Comparatively, the microstructural assessment of the MetalX^{TM} 17-4PH stainless steel demonstrated a predominately martensitic microstructure, with some reverted inter-lath austenite formed in the heat-affected areas throughout printing [23,36]. The reverted austenite induces the transformation-induced-plasticity (TRIP) effect, where austenite transforms to martensite throughout plastic deformation, resulting in reduced yield strength and increased ductility commonly among steels [42]. The non-lath austenitic regions are most evident in Scanning Electron Microscopy (SEM) imaging as displayed in Figure 3, contrasting the cast martensite microstructure in Figure 2 [23].

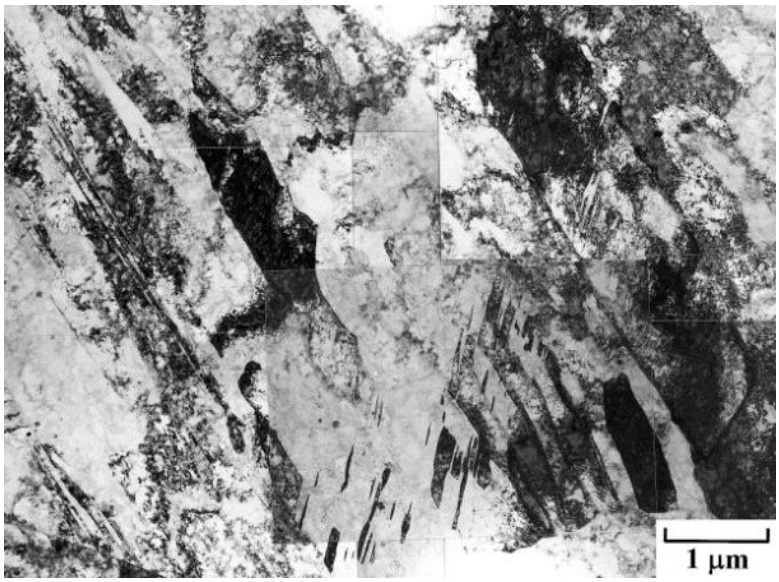

Figure 2. Cast TEM imaging of the martensite microstructure [13].

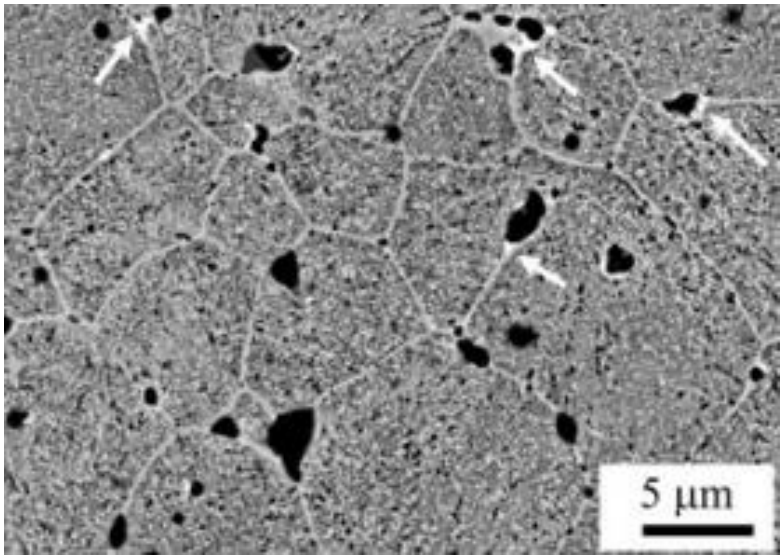

Figure 3. MetalX^{TM} SEM imaging of the reverted non-lath austenitic regions [23].

Energy Dispersive Spectroscopy (EDS) analysis identifies the formation of Niobium Carbide (NbC) precipitates up to 10 μm in size, responsible for high-stress sites and subsequent cracks. The NbC pores are commonly removed throughout homogenization; however, the sintering of the AM alloy has not achieved this [24]. Porosity analysis by SEM identified major defects including elongated pits and voids adjacent to deposited filaments, concluding poor infusion of the filaments throughout MetalX^{TM} printing [21,23,43,44]. Formation of the high porosity and large precipitates directly impact the strength and ductility of the MetalX^{TM} alloy, reducing the cross-sectional area for load bearing and inducing fracture. Furthermore, studies on the MetalX^{TM} alloy using different sinter cycles of corresponding parameters have observed variations in hardness, suggesting limitations to the printing process in achieving repeatability [26,33]. The surface roughness aligns with the print build layers at approximately 100 μm in height, owing to the 'stair stepping' effect fabricated naturally by the AM process. As surface roughness was identified to directly impact tensile strength, reduction of this phenomenon would be necessary to optimize mechanical performance [45,46]. It is further established the impact of process parameters on the mechanical strength produced by the MetalX^{TM} printer, identifying extrusion

temperature, infill rate, material flow, cooling rate post-printing, and build orientation to all contribute to the resultant microstructural characteristics, size, and placement of material defects [22,47]. Gonzalez-Gutierrez et al. [48] observed an optimized extrusion temperature of 260 °C, flow rate multiplier of 200%, and printing rate multiplier of 100% for 17-4PH Stainless Steel. The tensile strength findings included an average Young's modulus of 196 GPa, maximum stress of 696 MPa, and strain at break of 4%. Jagtap BM et al. investigated tensile strength relative to infill density of the ADAM 17-4PH Stainless Steel, finding that a weight reduction of 20% due to infill density translates to a reduction of 10–15% in tensile strength [47]. Analysis of defects relative to the build orientation demonstrates a correlation to defect geometry; print height angles of 0 to 10 degrees displayed triangular-shaped pores of small areas, 20 to 50 degrees displayed slightly larger diamond shaped pores, and 60 to 90 degree specimen displayed large rectangular pores as observed in Figure 4 [22,43].

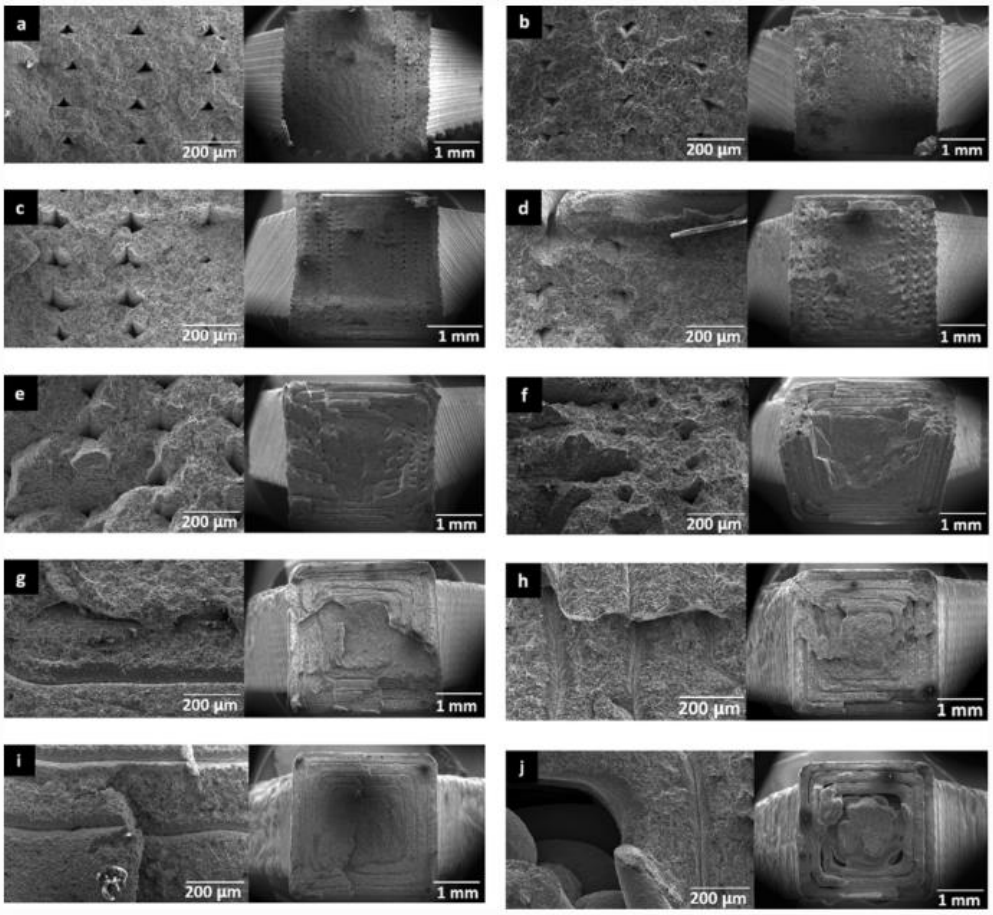

Figure 4. Cross-sectional SEM imaging of MetalX^{TM} specimens relative to print angle of (**a**) 0°, (**b**) 10°, (**c**) 20°, (**d**) 30°, (**e**) 40°, (**f**) 50°, (**g**) 60°, (**h**) 70°, (**i**) 80°, and (**j**) 90° [22].

The findings of the aforementioned paper suggest a defect geometry correlation to print angle, where the formation of air gaps is attributed to underfill between deposited toolpath lines of the walls [23]. The increased defect area is attributed to the lower mechanical performance in the 60° to 90° oriented MetalX^{TM} specimen, although no relationship between defect geometry and mechanical property performance has been investigated to date. The defect geometry shape is a function of specimen orientation relative to the build plate due to the underlying limitations of the technique's layer-by-layer fusion methodology. As the specimen orientation approaches a 60° angle, the defect geometry reaches a maximum volume, thus a minimal cross-sectional area is achieved, and the lowest tensile strengths are observed [22]. This holds for the specimen oriented until 90°, comprising similar defect

volumes of varying geometries. Research suggests increasing the flow rate multiplier or decreasing the layer thickness could reduce the presence of air gaps [23,49,50]; however, this has not been confirmed with the MetalX™ printer. Investigation into the material characteristics produced by alternate AM technologies demonstrates comparable material phases and high porosity to the MetalX™ system. 17-4PH Stainless Steel fabricated by Laser PBF identified a correlation in material phase to the type of powder; water-atomized powder consisted of martensite and austenite phases, whereas gas-atomized powder consisted only of martensite [19,26,33,34]. A reduction in porosity is seen in the alloy fabricated by MIM, achieving a δ-ferrite [26] chemical composition within the pore surface, resulting in high densification after sintering [37,38,43,47].

Microstructural analysis of the cast and MetalX™ 17-4PH stainless steel identified variance in microstructure phase and defect size. The MetalX™ alloy formed lath austenite in heat-affected areas, in comparison to, the cast alloy of the complete martensitic phase. With increasing porosity size and shape relative to print height, the MetalX™ alloy demonstrates anisotropic behavior in contrast to the wrought. Comparison to other AM technologies identifies the austenite formation relative to the AM process, requiring process parameter optimization relative to technique to reduce material defects, and subsequently improve mechanical performance.

4. Mechanical Property Performance Post-Heat Treatment

The mechanical properties of cast and AM 17-4PH stainless steel can be improved through the application of post-processing heat treatment, with a significant effect on most properties. The cast alloy has optimized mechanical performance through the application of the H900 heat treatment [18], involving exposure to a temperature of 482 °C for a duration of one hour. The resultant mechanical properties per the ASTM standard as given in Table 3; the particular increase is found in UTS, yield strength, and hardness, at 1310 MPa, 1170 MPa, and 40 HRC, respectively [19,20].

Table 3. Comparison of MetalX™, MIM, and wrought post-heat-treatment mechanical properties.

Mechanical Properties	Markforged H900 [20,21]	MIM H900 [18]	ASTM A564 H900 [20]
UTS	1230 MPa	1190 MPa	1310 MPa
0.2% Yield Strength	1050 MPa	1090 MPa	1170 MPa
Elongation at Break	13%	6%	10%
Tensile Modulus	170 GPa	190 GPa	190 GPa
Hardness	38 HRC	33 HRC	40 HRC
Relative Density	96.4%	95.5%	100%

Application of the H900 heat treatment to the MetalX™ 17-4PH stainless steel demonstrates a significant increase in corresponding properties, achieving strength and hardness close to the wrought, and a higher ductility by 3% as achieved by Markforged [20]. Table 3 also demonstrates the mechanical properties obtained by H900 application to MIM, achieving slightly improved properties in yield strength and Young's Modulus to the MetalX™ system, but performs lower in all other mechanical properties and density [20,41]. Akessa et al. [23] investigated the effect on the microstructure of the MetalX™ 17-4PH stainless steel by various heat treatments. Figure 5 displays the application of post-processing solution treatment and various direct aging heat treatments. All figures demonstrate the transformation of reverted austenite observed in the as-fabricated specimen to fully formed martensite attributing the higher performing mechanical properties [23].

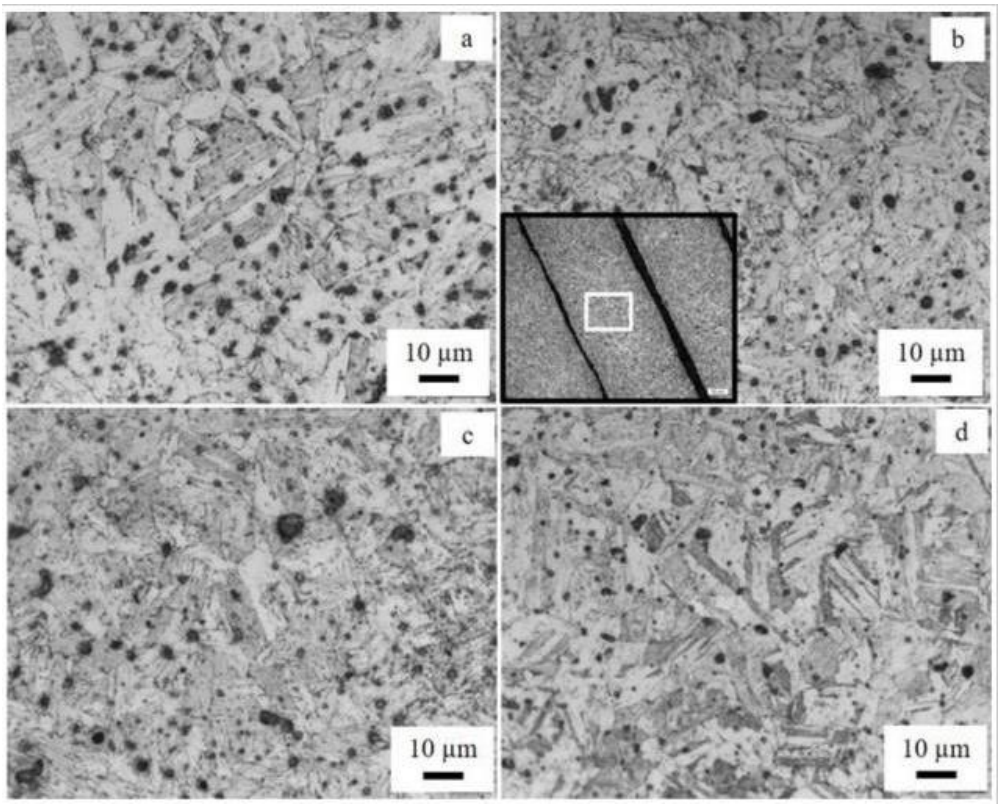

Figure 5. Light Optical Microscopy (LOM) of solution treated and direct aged heat treatments applied to the MetalX^{TM} 17-4PH stainless steel of (**a**) Solution Treatment, (**b**) Direct Aged, (**c**) Direct Aged, (**d**) Direct Aged [23].

Literature analysis of the MetalX^{TM} alloy's mechanical properties supports the Mark-forged values but records a high variance in results at much lower performances [24,33]. Investigation into optimizing the mechanical properties fabricated by MetalX^{TM} has identified the combination of HIP followed by direct aging to produce a maximal mechanical performance [21]. A relative density of up to 98.5% was recorded, yield strength of 1000 MPa, UTS of 1160 MPa, Young's modulus of 187 GPa, hardness of 44.7 HRC, and ductility of 7.5% elongation at fracture. Alternate studies have proven further improvement to mechanical properties with the application of the H900 heat treatment and refinement of printing parameters, producing a yield strength of 1113 MPa, UTS of 1346 MPa, and ductility of 7.8% elongation at fracture [45]. This study identified the formation of NbC and Copper-rich particle (CRP) precipitates due to the H900 precipitation environment of BCC crystal structure. Development of the NbC precipitates was found to reduce material porosity throughout sintering among other AM techniques, thus refining this material structure for the MetalX^{TM} system could lead to optimal porosity reduction [23,24,49]. The high variance in mechanical property performance observed from reviewing published literature highlights deficiencies in the MetalX^{TM} process. Therefore, no heat-treatment application guarantees reproducibility in property performance, and no conclusions can be drawn to identify the heat-treatment application that results in optimal mechanical properties.

5. Summary and Suggestions for Future Research

This review paper analyzed the as-fabricated properties of cast and MetalX^{TM} 17-4PH stainless steel in comparison to other AM techniques, the material microstructure, porosity, and mechanical property improvement through the application of post-processing heat treatment. The as-fabricated mechanical properties achieved by the MetalX^{TM} system had improved UTS and hardness to the wrought material but showed significant variance in Young's modulus, ductility, and porosity. In the as-fabricated state, AM demon-

strated competitive tensile strength, ductility, and hardness to the wrought counterpart. Analysis of the material characteristic indicated a fully martensitic microstructure developed in the cast alloy, whereas the MetalX^{TM} specimen showed a slight formation of an austenitic microstructure and significant porosity increasingly proportionate to the print angle. Anisotropic performance was established relative to print angle in contrast to the cast material; however, mechanical properties relative to build orientation are yet to be investigated. Thus, the anisotropic nature of the MetalX^{TM} alloy cannot be concluded. Slight development of the austenitic microstructure was commonly found in AM 17-4PH stainless steel, with porosity directly impacting the mechanical property performance. Development of the austenitic regions was attributed to heat-affected areas throughout the print process, yet there is no explanation to support this statement [23,24]. The AM alloy's properties can be improved through the application of post-processing heat treatment, achieving comparable mechanical performance to the wrought counterpart, and improved ductility. Refinement of process parameters in addition to heat treatment has shown AM to surpass wrought properties in UTS [51]. AM findings have demonstrated that adjusting parameters of flow rate multiplier or layer thickness can minimize porosity [23,35]; however, this has not been explored with the MetalX^{TM} printer. If the BPE process can achieve porosity reduction, optimization of these parameters could increase mechanical property performance greater than the cast counterpart.

The findings of this literature review have identified areas of further investigation into the reproducibility of the MetalX^{TM} system, refinement of process parameters, and application of post-processing heat treatment. In particular, an investigation into a reduction of porosity through adjustment of infill rate and layer thickness presents an opportunity to increase the mechanical property performance relative to all print angles, thus reducing the current anisotropic nature. Furthermore, refinement of the microstructure through adjustment of extrusion temperature may form fully developed martensite, corresponding to the cast microstructure. Achievement of this microstructure and reduction of porosity may reduce the high property variance observed in the literature. Furthermore, the investigation into post-processing heat treatment to support a fully developed martensite microstructure or complete reduction in porosity is necessary to optimize the mechanical properties. The high variance in as-fabricated properties limits current findings to the heat-treatment application; however, an increased sample size may develop over-arching trends relative to treatment temperature and exposure time, irrelative to the variance in as-fabricated properties.

The MetalX^{TM} system demonstrates the capability to be a competitive contender to the mechanical performance produced by casting. Refinement of the processing parameters is required for optimization of the material properties, reducing defect quantity and size. Furthermore, the application of heat treatment shows a significant increase in mechanical property performance and material homogenization. This presents a significant opportunity for further investigation into the impact of individual process parameters on the material characteristics and porosity to optimize the fusion of print layers. Additionally, further investigation into a wider variance in heat-treatment application will identify the optimal post-processing conditions to achieve results closer to, or surpassing the wrought material.

Author Contributions: Conceptualization, R.H.; formal analysis, J.J.; investigation, J.J., A.V. and R.H.; data curation, J.J.; writing—original draft preparation, J.J.; writing—review and editing, R.H. and A.V.; visualization, J.J.; supervision, R.H. and A.V.; project administration, R.H. All authors have read and agreed to the published version of the manuscript.

Funding: This research received no external funding.

Data Availability Statement: No new data were created.

Conflicts of Interest: The authors declare no conflict of interest.

References

1. Van Sice, C.; Faludi, J. Comparing environmental impacts of metal additive manufacturing to conventional manufacturing. *Proc. Des. Soc.* **2021**, *1*, 671–680. [CrossRef]
2. Javaid, M.; Haleem, A.; Singh, R.P.; Suman, R.; Rab, S. Role of additive manufacturing applications towards environmental sustainability. *Adv. Ind. Eng. Polym. Res.* **2021**, *4*, 312–322. [CrossRef]
3. Kuz'min, M.P.; Kuz'mina, M.Y.; Kuz'mina, A.S. Production and properties of aluminum-based composites modified with carbon nanotubes. *Mater. Today Proc.* **2019**, *19*, 1826–1830. [CrossRef]
4. Monzón, M.D.; Ortega, Z.; Martínez, A.; Ortega, F. Standardization in additive manufacturing: Activities carried out by international organizations and projects. *Int. J. Adv. Manuf. Technol.* **2015**, *76*, 1111–1121. [CrossRef]
5. Vafadar, A.; Guzzomi, F.; Rassau, A.; Hayward, K. Advances in Metal Additive Manufacturing: A Review of Common Processes, Industrial Applications, and Current Challenges. *Appl. Sci.* **2021**, *11*, 1213. [CrossRef]
6. Suwanpreecha, C.; Seensattayawong, P.; Vadhanakovint, V.; Manonukul, A. Influence of specimen layout on 17-4PH (AISI 630) alloys fabricated by low-cost additive manufacturing. *Metall. Mater. Trans. A* **2021**, *52*, 1999–2009. [CrossRef]
7. Pérez, M.; Carou, D.; Rubio, E.M.; Teti, R. Current advances in additive manufacturing. *Procedia CIRP* **2020**, *88*, 439–444. [CrossRef]
8. Tavares, S.S.M.; Da Silva, F.; Scandian, C.; Da Silva, G.; De Abreu, H. Microstructure and intergranular corrosion resistance of UNS S17400 (17-4PH) stainless steel. *Corros. Sci.* **2010**, *52*, 3835–3839. [CrossRef]
9. Lai, Z.; Wang, C.; Zheng, L.; Lin, H.; Yuan, Y.; Yang, J.; Xiong, W. Effect of cryogenic oils-on-water compared with cryogenic minimum quantity lubrication in finishing turning of 17-4PH stainless steel. *Mach. Sci. Technol.* **2020**, *24*, 1016–1036. [CrossRef]
10. Emygdio, G.; Zeemann, A. *Failures of 17-4 PH Steel Parts in Non Sour Environments*; OnePetro: San Antonio, TX, USA, 2014.
11. Prakash, K.S.; Nancharaih, T.; Rao, V.S. Additive manufacturing techniques in manufacturing-an overview. *Mater. Today Proc.* **2018**, *5*, 3873–3882. [CrossRef]
12. Ran, X.-z.; Liu, D.; Li, J.; Liu, X.; Wang, H.-m.; Cheng, X.; He, B.; Tang, H.-b. Effects of post homogeneity heat treatment processes on microstructure evolution behavior and tensile mechanical properties of laser additive manufactured ultrahigh-strength AerMet100 steel. *Mater. Sci. Eng. A* **2018**, *723*, 8–21. [CrossRef]
13. Hsiao, C.; Chiou, C.; Yang, J. Aging reactions in a 17-4 PH stainless steel. *Mater. Chem. Phys.* **2002**, *74*, 134–142. [CrossRef]
14. Lotfizarei, Z.; Mostafapour, A.; Barari, A.; Jalili, A.; Patterson, A.E. Overview of debinding methods for parts manufactured using powder material extrusion. *Addit. Manuf.* **2022**, *61*, 103335. [CrossRef]
15. Kauffmann, J.; Chemkhi, M.; Gardan, J. Integrated design and dimensional compliance of Bound Powder Extrusion technology: A case study of an aircraft engine bracket. *Procedia CIRP* **2022**, *108*, 158–163. [CrossRef]
16. Bouaziz, M.; Djouda, J.M.; Chemkhi, M.; Rambaudon, M.; Kauffmann, J.; Hild, F. Heat treatment effect on 17-4PH stainless steel manufactured by Atomic Diffusion Additive Manufacturing (ADAM). *Procedia CIRP* **2021**, *104*, 935–938. [CrossRef]
17. Bazri, S.; Mapelli, C.; Barella, S.; Gruttadauria, A.; Mombelli, D.; Liu, C. Mechanical and tribo-metallurgical behavior of 17-4 precipitation hardening stainless steel affected by severe cold plastic deformation: A comprehensive review article. *J. Braz. Soc. Mech. Sci. Eng.* **2022**, *44*, 247. [CrossRef]
18. Incorporated, A.T. Technical Data Sheet. Online; ATI 425. 2014. Available online: atimaterials.com (accessed on 4 July 2023).
19. Rack, H. *Physical and Mechanical Properties of Cast 17-4 PH Stainless Steel*; Sandia National Labs.: Albuquerque, NM, USA, 1981.
20. Markforged. Material Data Sheet. Online. 2022. Available online: markforged.com (accessed on 4 July 2023).
21. Sambrook, C. *The Effect of Heat Treatment and Print Direction on Additively Manufactured 17-4 PH Stainless Steel*; UQ esSpace, University of Queensland, Australia: Brisbane, QLD, Australia, 2021.
22. Alkindi, T.; Alyammahi, M.; Susantyoko, R.A.; Atatreh, S. The effect of varying specimens' printing angles to the bed surface on the tensile strength of 3D-printed 17-4PH stainless-steels via metal FFF additive manufacturing. *MRS Commun.* **2021**, *11*, 310–316. [CrossRef]
23. Dareh Baghi, A.; Nafisi, S.; Hashemi, R.; Ebendorff-Heidepriem, H.; Ghomashchi, R. Machining Versus Heat Treatment in Additive Manufacturing of Ti6Al4V Alloy. In *The Minerals, Metals & Materials Series*; Springer International Publishing: Anaheim, CA, USA, 2022; pp. 187–197.
24. Irrinki, H.; Nath, S.D.; Alhofors, M.; Stitzel, J.; Gulsoy, O.; Atre, S.V. Microstructures, properties, and applications of laser sintered 17-4PH stainless steel. *J. Am. Ceram. Soc.* **2019**, *102*, 5679–5690. [CrossRef]
25. Abe, Y.; Kurose, T.; Santos, M.V.; Kanaya, Y.; Ishigami, A.; Tanaka, S.; Ito, H. Effect of layer directions on internal structures and tensile properties of 17-4PH stainless steel parts fabricated by fused deposition of metals. *Materials* **2021**, *14*, 243. [CrossRef]
26. Irrinki, H.; Jangam, J.S.D.; Pasebani, S.; Badwe, S.; Stitzel, J.; Kate, K.; Gulsoy, O.; Atre, S.V. Effects of particle characteristics on the microstructure and mechanical properties of 17-4 PH stainless steel fabricated by laser-powder bed fusion. *Powder Technol.* **2018**, *331*, 192–203. [CrossRef]
27. Zhang, Y.; Roch, A. Fused filament fabrication and sintering of 17-4PH stainless steel. *Manuf. Lett.* **2022**, *33*, 29–32. [CrossRef]
28. Akessa, A.D.; Tucho, W.M.; Lemu, H.G.; Grønsund, J. Investigations of the Microstructure and Mechanical Properties of 17-4 PH ss Printed Using a MarkForged Metal X. *Materials* **2022**, *15*, 6898. [CrossRef]
29. Henry, T.C.; Morales, M.A.; Cole, D.P.; Shumeyko, C.M.; Riddick, J.C. Mechanical behavior of 17-4 PH stainless steel processed by atomic diffusion additive manufacturing. *Int. J. Adv. Manuf. Technol.* **2021**, *114*, 2103–2114. [CrossRef]
30. Burgess, A.; Dodd, R.; Radwani, M.; Opoz, T.; Tammas-Williams, S. *The Properties of Stainless Steel 17-4PH Produced by a Low-Cost Additive Manufacturing Technique, the Markforged MetalX™*; IOP Publishing: Liverpool, UK, 2022.

31. Suwanpreecha, C.; Manonukul, A. A review on material extrusion additive manufacturing of metal and how it compares with metal injection moulding. *Metals* **2022**, *12*, 429. [CrossRef]
32. Bianchi, I.; Di Pompeo, V.; Mancia, T.; Pieralisi, M.; Vita, A. Environmental impacts assessment of Bound Metal Deposition 3D printing process for stainless steel. *Procedia CIRP* **2022**, *105*, 386–391.
33. Sabooni, S.; Chabok, A.; Feng, S.C.; Blaauw, H.; Pijper, T.C.; Yang, H.J.; Pei, Y.T. Laser powder bed fusion of 17–4 PH stainless steel: A comparative study on the effect of heat treatment on the microstructure evolution and mechanical properties. *Addit. Manuf.* **2021**, *46*, 2214–8604. [CrossRef]
34. Irrinki, H.; Dexter, M.; Barmore, B.; Enneti, R.; Pasebani, S.; Badwe, S.; Stitzel, J.; Malhotra, R.; Atre, S.V. Effects of powder attributes and laser powder bed fusion (L-PBF) process conditions on the densification and mechanical properties of 17-4 PH stainless steel. *Jom* **2016**, *68*, 860–868. [CrossRef]
35. Gonzalez-Gutierez, J.; Godec, D.; Guráň, R.; Spoerk, M.; Kukla, C.; Holzer, C. 3D Printing conditions determination for feedstock used in fused filament fabrication (FFF) of 17-4ph stainless steel parts. *Metalurgija* **2017**, *57*, 117–120.
36. Lavecchia, F.; Pellegrini, A.; Galantucci, L.M. Comparative study on the properties of 17-4 PH stainless steel parts made by metal fused filament fabrication process and atomic diffusion additive manufacturing. *Rapid Prototyp. J.* **2022**, *29*, 393–407. [CrossRef]
37. Wu, M.-W.; Huang, Z.-K.; Tseng, C.-F.; Hwang, K.-S. Microstructures, mechanical properties, and fracture behaviors of metal-injection molded 17-4PH stainless steel. *Met. Mater. Int.* **2015**, *21*, 531–537. [CrossRef]
38. Seerane, M.; Machaka, R. *Metal Injection Moulding of 17-4PH Stainless Steel: Effects of Porosity on the Mechanical Properties of the Sintered Products*; IOP Publishing: Riverside Run, South Africa, 2019.
39. Susan, D.; Crenshaw, T.; Grant, R.; Kilgo, A.; Wright, R. Effect of porosity on ductility variation in investment cast 17-4PH. *Microsc. Microanal.* **2005**, *11*, 1664–1665. [CrossRef]
40. Hilditch, T.; De Souza, T.; Hodgson, P. Properties and automotive applications of advanced high-strength steels (AHSS). In *Welding and Joining of Advanced High Strength Steels (AHSS)*; Elsevier: Amsterdam, The Netherlands, 2015; pp. 9–28.
41. Susan, D.; Crenshaw, T.; Gearhart, J. The effects of casting porosity on the tensile behavior of investment cast 17-4PH stainless steel. *J. Mater. Eng. Perform.* **2015**, *24*, 2917–2924. [CrossRef]
42. Adamczyk-Cieślak, B.; Koralnik, M.; Kuziak, R.; Majchrowicz, K.; Zygmunt, T.; Mizera, J. The Impact of Retained Austenite on the Mechanical Properties of Bainitic and Dual Phase Steels. *J. Mater. Eng. Perform.* **2022**, *31*, 4419–4433. [CrossRef]
43. Singh, G.; Missiaen, J.-M.; Bouvard, D.; Chaix, J.-M. Additive manufacturing of 17-4 PH steel using metal injection molding feedstock: Analysis of 3D extrusion printing, debinding and sintering. *Addit. Manuf.* **2021**, *47*, 102287. [CrossRef]
44. Raju, N.; Warren, P.; Subramanian, R.; Ghosh, R.; Raghavan, S.; Fernandez, E.; Kapat, J. *Material Properties of 17-4PH Stainless Steel Fabricated by Atomic Diffusion Additive Manufacturing (ADAM)*; University of Texas at Austin: Austin, TX, USA, 2021.
45. Delfs, P.; Toews, M.; Schmid, H.-J. *Surface Roughness Optimized Alignment of Parts for Additive Manufacturing Processes*; University of Texas at Austin: Austin, TX, USA, 2015.
46. Mahamood, R.M.; Akinlabi, E.T.; Shukla, M.; Pityana, S. Revolutionary Additive Manufacturing: An Overview. *Lasers Eng.* **2014**, *27*, 161–178.
47. Jagtap, B.M.; Kakandikar, G.M.; Jawade, S.A. Mechanical Behavior of Inconel 625 and 17-4 PH Stainless Steel Processed by Atomic Diffusion Additive Manufacturing. In *Recent Advances in Manufacturing Processes and Systems: Select Proceedings of RAM 2021*; Springer: Singapore, 2022; pp. 583–594.
48. Gonzalez-Gutierreza, J.; Florian, A.; Schlaufc, T.; Kuklad, C.; Holzera, C. Tensile properties of sintered 17-4PH stainless steel fabricated by material extrusion additive manufacturing. *Mater. Lett.* **2019**, *248*, 165–168. [CrossRef]
49. Rankouhi, B.; Javadpour, S.; Delfanian, F.; Letcher, T. Failure analysis and mechanical characterization of 3D printed ABS with respect to layer thickness and orientation. *J. Fail. Anal. Prev.* **2016**, *16*, 467–481. [CrossRef]
50. Cho, Y.-H.; Park, S.-Y.; Kim, J.-Y.; Lee, K.-A. 17-4PH stainless steel with excellent strength–elongation combination developed via material extrusion additive manufacturing. *J. Mater. Res. Technol.* **2023**, *24*, 3284–3299. [CrossRef]
51. Dareh Baghi, A.; Nafisi, S.; Hashemi, R.; Ebendorff-Heidepriem, H.; Ghomashchi, R. A New Approach to Empirical Optimization of Laser Powder Bed Fusion Process for Ti6Al4V Parts. *J. Mater. Eng. Perform.* **2023**, 1–17. [CrossRef]

Disclaimer/Publisher's Note: The statements, opinions and data contained in all publications are solely those of the individual author(s) and contributor(s) and not of MDPI and/or the editor(s). MDPI and/or the editor(s) disclaim responsibility for any injury to people or property resulting from any ideas, methods, instructions or products referred to in the content.